Eur Biophys J (1997) 26: 195–201 

ARTICLE

**E. C. Reynhardt**

# The role of hydrogen bonding in the cuticular wax of *Hordeum vulgare* L.

Received: 6 February 1997 / Accepted: 24 February 1997

**Abstract** The role of hydrogen bonding in the cuticular wax of *Hordeum vulgare* L. has been investigated by comparing differential scanning calorimetry and X-ray powder diffraction results of the wax with those of *n*-alkane mixtures with chain-length distributions resembling that of the wax. It is concluded that hydrogen bonding prevents separation of the short and long chain-length distributions and results in the formation of an amorphous component which is large compared with that of a typical paraffinic wax. It seems that the longer ester chains ($39 \geq n \geq 50$) bridge the amorphous zone containing chain-ends between two adjacent layers of shorter chains ($20 \geq n \geq 33$), where $n$ is the number of carbon atoms per chain. In contrast to a paraffinic wax, which has a monolayered structure, this plant wax has a bilayered structure.

**Key words** Cuticular wax · Hydrogen bonding · Crystallinity · Structure

## 1 Introduction

The plant cuticle serves as a protective barrier to the environment, controlling excessive water and nutrient losses. The matrix of this extracellular lipophilic membrane consists of the bipolymer cutin which is essentially an amorphous polyester of hydroxyalkanoic acids (Kolattukudy 1980; Holloway 1982). Cuticular waxes embedded within this matrix and deposited on its outer surface, consist of a mixture of long-chain aliphatic components (Baker 1982).

Waxes from the leaves of *Citrus aurantium* L., *Fagus sylvatica* L. (European beech tree) and *Hordeum vulgare* L. (barley) have been investigated using. NMR, DSC, X-ray diffraction and gas chromatography methods (Reynhardt and Riederer 1991, 1994). These waxes have chain-length distributions which can be described as the superposition of two distinct chain-length distributions, one centered around ~26 carbon atoms and the other around ~46 carbon atoms. The shorter chain-length distribution consists of *n*-alkanals, *n*-alkanes, *n*-alkanoic acids and *n*-alkanols, while the longer distribution is made up of *n*-alkyl esters.

The main structural difference between a paraffinic wax, consisting of *n*-alkanes with a distribution of chain-lengths (Reynhardt 1985a, b, 1986), and a plant wax is the presence of intermolecular hydrogen bonds in the latter. In the case of *n*-alkanes the interchain forces are relatively weak van der Waals forces without any hydrogen bonding, while the presence of alkanals, acids, alkanols and esters in plant waxes leads to intermolecular hydrogen bonds. In this paper the effect of hydrogen bonding in plant waxes is investigated by comparing X-ray powder diffractograms and thermograms of *Hordeum vulgare* wax with those obtained for *n*-alkane mixtures with similar chain-length distributions. It is shown that hydrogen bonding in plant waxes prevents phase separation of the shorter and longer chain distributions, reduces the crystallinity and increases the melting point of the wax.

E. C. Reynhardt (✉)
Department of Physics, University of South Africa, PO Box 392, Pretoria 0001, South Africa

## 2 Experimental

*n*-Alkane samples, *n*-$C_nH_{2n+2}$ (abbreviated as $C_n$), with stated purities >98%, were obtained from Fluka GMBh and were used without purification.

The following samples were prepared:

– $C_{26}$ and $C_{46}$ as supplied
– A binary mixture $C_{26}C_{46}$ with a mass ratio (9:1)
– An *n*-alkane multiple mixture (Mm1) with $34 \geq n \geq 20$ and $\bar{n} = 26$
– An *n*-alkane multiple mixture (Mm2) with $48 \geq n \geq 40$ and $\bar{n} = 46$
– An *n*-alkane multiple mixture (Mm3) with $48 \geq n \geq 20$, resembling the chain-length distribution of *Hordeum vulgare* wax.

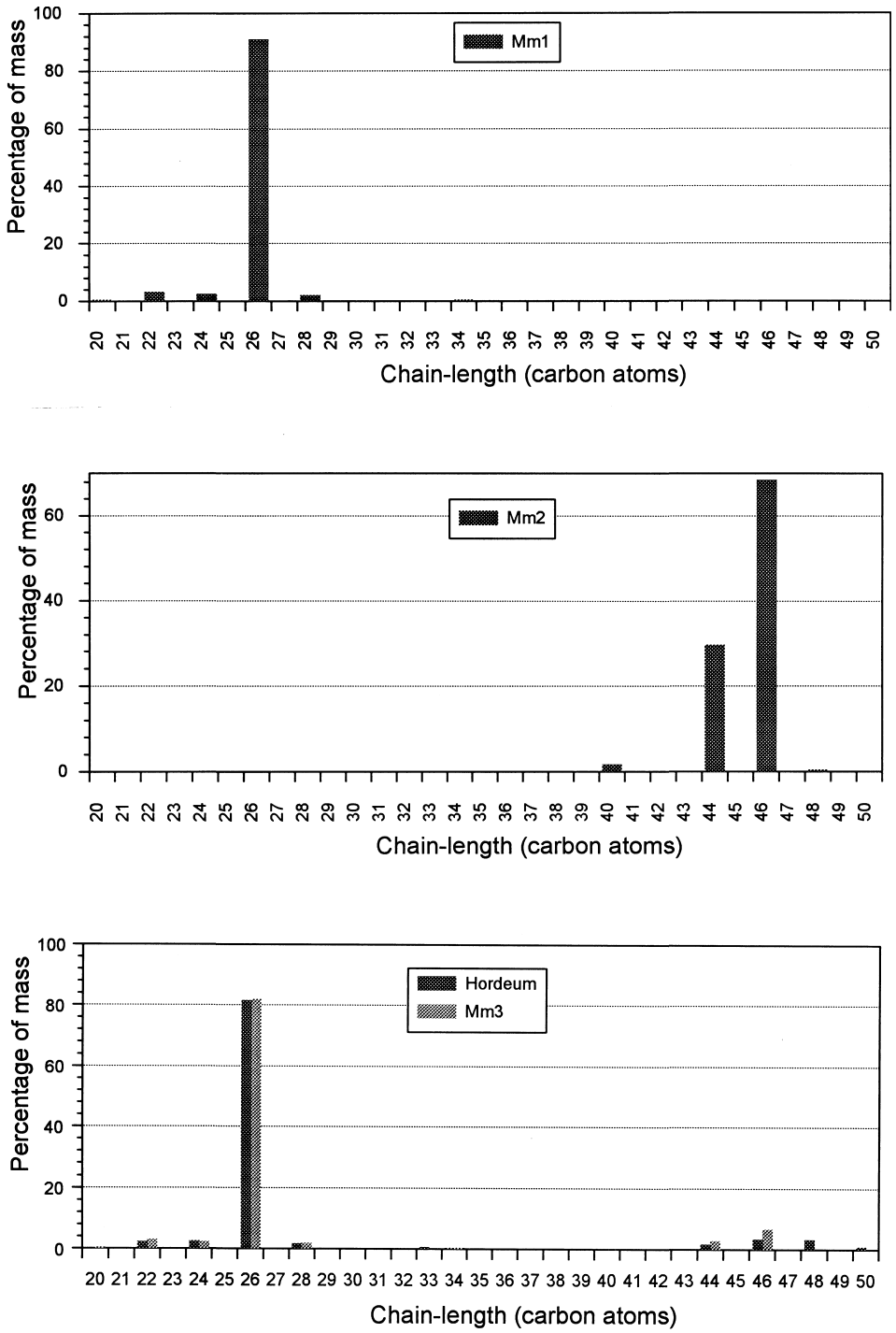


**Fig. 1** Chain-length distributions of the multiple mixtures of *n*-alkanes and *Hordeum vulgare* wax.

The chain-length distributions of the multiple mixtures are shown in Fig. 1.

Plants of *Horedeum vulgare* L. (cultivar Andrea) were cultivated in growth chambers under controlled conditions. Fully developed leaves were harvested when the plants had more than three leaves unfolded but did not yet start tillering.

The plant wax sample used in this investigation was the same one used by Reynhardt and Riederer (1994). Cuticular wax was extracted from whole leaves as described by Riederer and Schneider (1990) by immersing the leaf blades in chloroform (>99%) for 30 min at 303 K. Average extraction efficiencies were about 90% of the total wax present in fresh leaves. The analysis of the cuticular wax components was described previously (Reynhardt and Riederer 1994). The chain-length distribution of the wax is shown in Fig. 1.

Diffraction data were collected on a Siemens D5000 powder diffractometer, using Cu K$\alpha$ radiation and reflec-

tion geometry. The diffractometer is equipped with a PSD detector. The scanning speed was 10 s per 2 $\theta$ degree.

Thermograms were recorded on a Stanton Redcroft DSC700. Heating rates were 5 K/min.

## 3 Results and discussion

### 3.1 Lamellar thickness

The lamellar thickness of a monolayered compound, like an *n*-alkaline, mixture of *n*-alkanes or a wax can be obtained from an X-ray diffractogram by using

$$L = \frac{m\lambda}{2 \sin \theta}, \quad (1)$$

where $\lambda$ is the wavelength of the radiation, $2\theta$ is the diffraction angle and $m$ is the order of the diffraction from the layer surfaces. By using

$$L = 1.27n + \delta, \quad (2)$$

where $\delta$ is an end-correction determined by the width of the chain-length distribution (Stokhuyzen and Pistorius 1970; Basson and Reynhardt 1992a), one can determine the average chain-length. For *n*-alkanes $\delta = 0.94$ Å (Nyburg and Potworowski 1973), while it is ~1.27 Å for wax fractions with a narrow chain-length distribution (Stockhuyzen and Pistorius 1970). From X-ray studies of multiple mixtures of *n*-alkanes (Basson and Reynhardt 1992a) it follows that

$$\delta = 0.33\ \sigma + 0.55, \quad (3)$$

where $\sigma$ is the standard deviation from the mean chain-length.

### 3.2 Normal alkanes

The thermograms of the above-mentioned samples and *Hordeum vulgare* wax are shown in Fig. 2. The solid-solid transition temperatures and the melting points are listed in Table 1 and the measured and calculated $L$ values and chain-length statistics for the different samples are listed in Table 2.

The observed $L = 31.1 \pm 1.0$ Å for $C_{26}$ is in close agreement with the value of 30.95 Å calculated and observed by Nyburg and Potworowski (1973) for a monoclonic unit cell. Craig et al. (1994) pointed out that this structure may be triclinic, but this debate is of no consequence as far as the present investigation is concerned. The observed $L = 60.6 \pm 1.0$ Å for $C_{46}$ is in reasonable agreement with $L = 61.97$ Å revealed by high-resolution synchrotron X-ray powder diffraction (Craig et al. 1994).

The melting points of $C_{26}$ and $C_{46}$ are 352 K and 363 K, respectively. The transition to the hexagonal phase of $C_{26}$ occurs at ~328 K. In this phase the chains rotate about their long axes (Reynhardt 1985a).

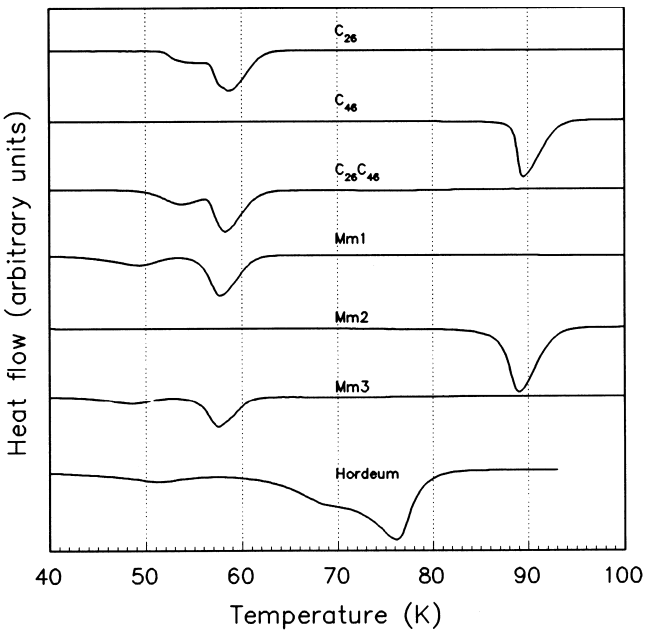


**Fig. 2** DSC thermograms of *n*-alkane mixtures and *Hordeum vulgare* wax.

**Table 1** Transition temperatures of *n*-alkanes, mixtures of *n*-alkanes and *Hordeum vulgare* wax

| Compound | Solid-solid transition (K) | Melting point (K) |
|---|---|---|
| $C_{26}$ | 328 | 332 |
| $C_{46}$ | | 363 |
| $C_{26}C_{46}$ | 327 | 331 |
| Mm1 | 322 | 331 |
| Mm2 | | 362 |
| Mm3 | 322 | 331 |
| *Hordeum* wax | 324, 342 | 349 |

**Table 2** Chain-length statistics of *n*-alkane mixtures and *Hordeum vulgare* wax

| Sample | $\bar{n}$ (carbon atoms) | $\sigma$ (carbon atoms) | $\delta$ (Å) | $L_{calc}$ (Å) | $L_{obs}$ (Å) |
|---|---|---|---|---|---|
| $C_{26}$ | 26 | – | 0.9 | 32.8 | 31.1 ± 1.0 |
| $C_{46}$ | 46 | – | 0.9 | 59.3 | 60.6 ± 1.0 |
| $C_{26}C_{46}$ | 27.2 | 4.8 | 2.0 | 36.5 | 31.2 ± 1.0 |
| | | | | | 60.7 ± 1.0 |
| Mm1 | 25.8 | 1.1 | 0.9 | | 31.1 ± 1.0 |
| | | | | 34 | 35.4 ± 1.0 |
| Mm2 | 45.3 | 1.2 | 0.9 | 59 | 60.4 ± 1.0 |
| Mm3 | 26.6 | 3.8 | 1.8 | | 33.1 ± 1.0 |
| | | | | 36 | 35.5 ± 1.0 |
| | | | | | 61.1 ± 1.0 |
| *Hordeum* wax | 27.1 | 3.8 | 1.8 | 36 | 77.5 ± 1.0 |

The calculated lamellar thickness of ~37 Å is not observed on the diffractogram of the binary mixture. However, the lamellar thicknesses of pure $C_{26}$ and $C_{46}$ are revealed by the diffractogram and it is concluded that the $C_{26}$

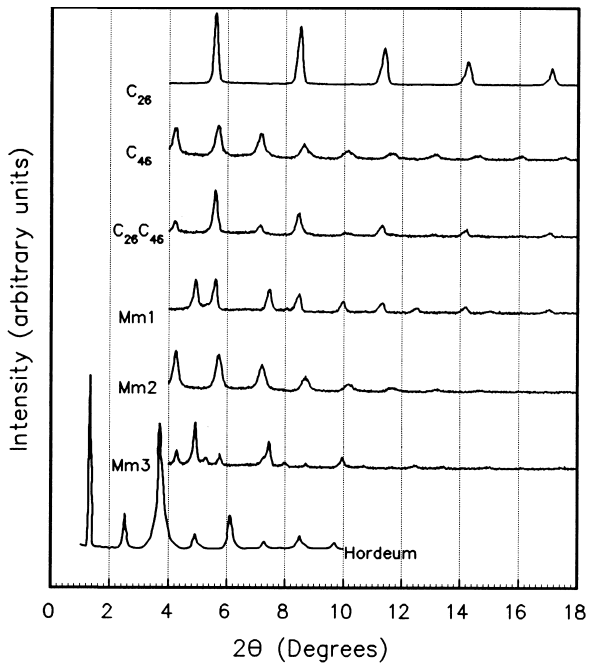


**Fig. 3** X-ray powder diffractograms of *n*-alkane mixtures and *Hordeum vulgare* wax.

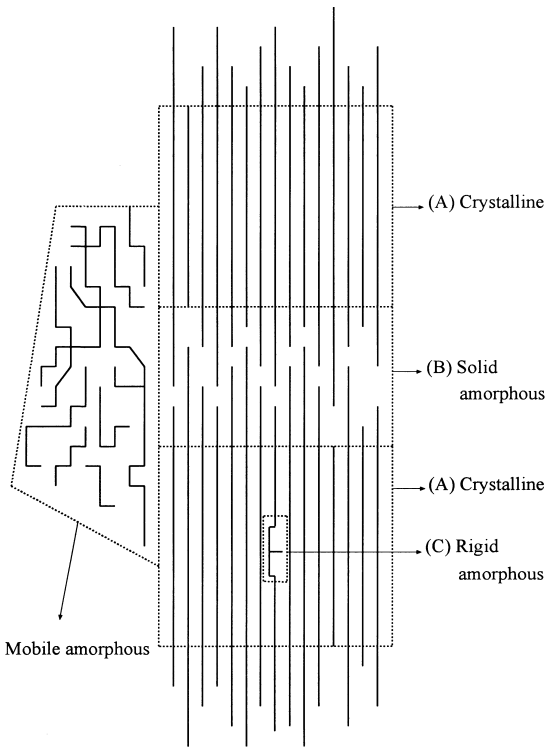


**Fig. 4** Representation of the structure of a wax with a normal distribution of chain-lengths. The different zones are discussed in the text

and $C_{46}$ phase separate during crystallization (Fig. 3). The monoclinic-hexagonal phase transition and the melting transition of $C_{26}$ are present on the thermogram, but the melting transition of $C_{46}$ is not observable. The explanation for this phenomenon is that since the $C_{26}$ and $C_{46}$ phases are separated, the $C_{26}$ phase melts first and then serves as a solvent for the $C_{46}$ phase which has dissolved totally in the liquid $C_{26}$ phase before its melting point at 363 K is reached.

The solid-solid phase transition of multiple mixture Mm1 occurs ~6 K lower than in the pure $C_{26}$ sample. However, the melting transition occurs at about the same temperature (331 K). Apart from the lamellar thickness of 31.1 Å, corresponding to the monoclinic structure of $C_{26}$, a second lamellar thickness $L = 35.4 \pm 1.0$ Å is observed on the diffractogram. Usually mixtures of *n*-alkanes and waxes have orthorhombic structures. However, since the Mm1 sample contain more than 90% $C_{26}$, it seems that domains of $C_{26}$ with the monoclinic structure and domains with a mixture of chains and the orthorhombic structure crystallise.

The diffractogram and thermogram of Mm2 are similar to those of $C_{46}$. The structure is also orthorhombic with the same lamellar thickness.

The thermogram of the Mm3 mixture is similar to that of Mm1. The melting of the long component (Mm2) is not observed. It seems that, as in the case of the binary mixture, phase separation occurs. The sample separates into two components, Mm1 and Mm2, and after Mm1 has melted, it acts as a solvent for Mm2. Therefore the melting of Mm2 is not observed on the thermogram. The dominant phase on the diffractogram is the structure of Mm1 with $L = 35.5$ Å. Two additional structures with $L$ values of 61 Å and 33 Å are observed. However, only small fractions of the sample belong to these structures. The former value corresponds to the observed lamellar thickness of Mm2.

### 3.3 Hordeum wax

The structure of a wax can be described in terms of crystalline and amorphous zones (Basson and Reynhardt 1992b; Reynhardt and Riederer 1994). The chain molecules are stacked in a regular fashion in the crystalline zone A, as shown in Fig. 4. The distribution in chain-lengths results in an amorphous region B between the chain ends of adjacent layers of chains and a liquid amorphous zone surrounding the crystallites. Since the chains of a plant wax consist of a number of different compounds, the crystalline zone cannot be perfectly crystalline. Differences in the chains lead to steric hindrances and disruption of the geometric homogeneity of the structure. A molecule tends to coil in a variable fashion under these circumstances, since the conditions do not allow it to maintain periodicity in any direction (Vainshtein 1966). Such molecules cannot form crystal structures for which identical units are required. This process contributes towards the amorphous zone of the plant wax and explains the relatively low crystallinity of plant and other oxidized waxes

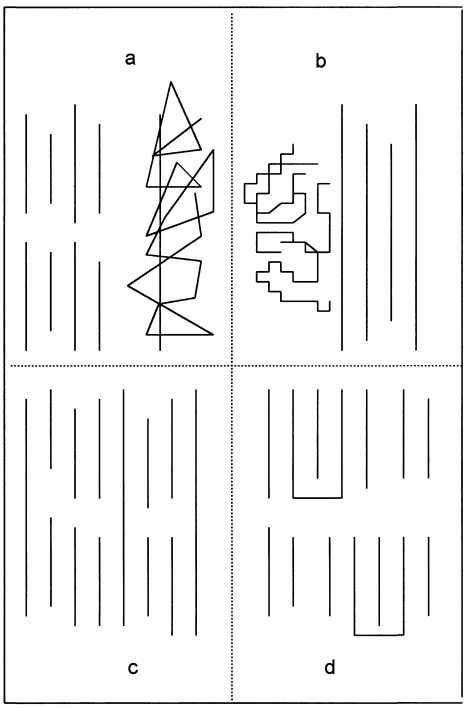


**Fig. 5** Representation of the different models for the crystallization of *Hordeum vulgare* wax. Models 1 to 4, discussed in the text, correspond to figures a to d, respectively

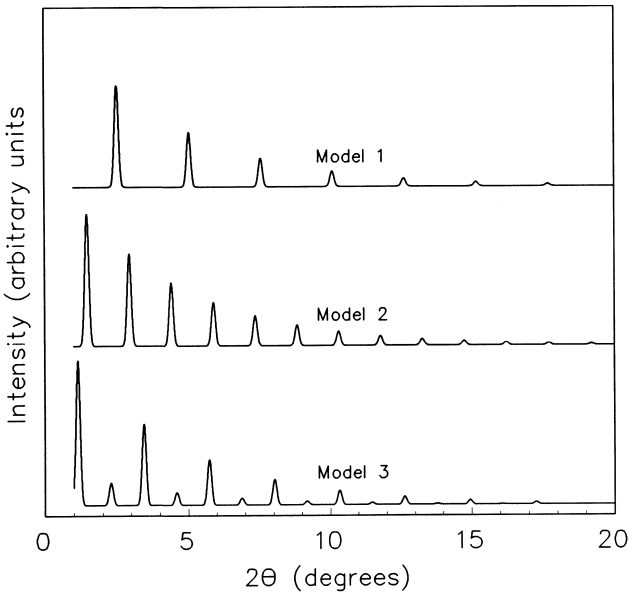


**Fig. 6** Simulated X-ray powder diffractograms for the different models for the structure of *Hordeum vulgare* wax.

compared with paraffinic waxes (~80%) (Le Roux and Loubser 1980). The crystalline zone of a plant wax contains those regions where a reasonable periodicity occurs. Rigid amorphous zones C occur within the crystalline zone and represent regions where the symmetry of the unit cell is violated, inter alia by side chains.

Crystallization from a saturated solution or from the melt may result in a number of different structures, as illustrated in Fig. 5.

*Model 1.* Shorter chains may crystallize into a separate zone, similar to Mm1, but with hydrogen bonds between adjacent chains. The longer ester chains could form a separate crystalline zone, similar to Mm2, or could be part of the amorphous zone (Fig. 5a).

*Model 2.* The long ester chains may form a crystalline zone, with the shorter chains in the amorphous zone (Fig. 5b).

*Model 3.* The long ester chains may be oriented parallel to the shorter chains and run through two adjacent layers of short chains. Such chains would form hydrogen bonds with the shorter chains (Fig. 5c).

*Model 4.* By folding an ester chain could be limited to a single layer of shorter chains. Such a folded chain can form hydrogen bonds with adjacent shorter chains (Fig. 5d).

The diffractogram of *Hordeum vulgare* wax shows a number of relatively weak 00*l* refections which belong to a single crystalline zone with $L = 77 \pm 2$ Å. This lamellar thickness is more than twice the calculated value for a mixture of chain-lengths forming a monolayered structure. Since the lamellar thickness can easily accommodate the longest chains (50 carbon atoms) in the wax (Reynhardt and Riederer 1994), it seems that the long ester chains determine the lamellar thickness and are therefore part of the crystalline zone. However, the crystallinity of *Hordeum* wax (~52% (Reynhart and Riederer 1994)) is much higher than the ester content (~10%), implying that the shorter chains contribute heavily to the crystalline zone. Therefore, it seems that Model 3, in which the long ester chains bridge the amorphous zone between two adjacent layers of shorter chains (Fig. 5c), thus forming a bilayered compound, is in agreement with the observed diffractogram. Figure 6 shows the simulated diffractograms for Models 1 (and 4), 2 and 3. The WYRIET program for Rietveld refinement of X-ray powder diffraction data (Schneider 1987) was used to generate these diffractograms. For the diffractogram of Model 3 every third chain was a long chain bridging the region between two adjacent short chain layers. It is interesting to note that the alternating strong and weak reflections are in qualitative agreement with the observed diffractogram of *Hordeum vulgare* wax.

An important observation is that the lamellar thickness is noticeably longer than the calculated value for a double layer of shorter chains (~68 Å). An explanation for this discrepancy is that $\delta$ for the plant wax is much greater than for monolayered *n*-alkane mixtures and waxes. From the average chain-length of the shorter chain-length distribution and the observed $L$ value for the wax, it is estimated

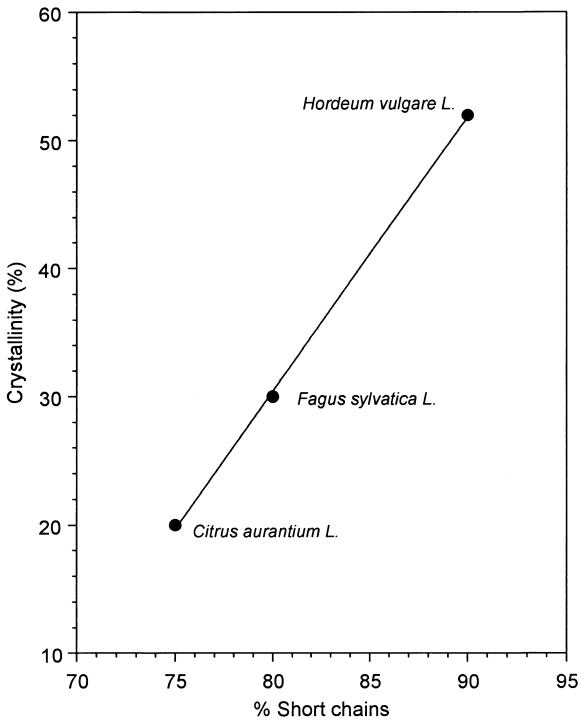


**Fig. 7** Crystallinity of three plant waxes as a function of percentage short chains in the wax. Data from Reynhardt and Riederer (1991, 1994) and present work

that $\delta \simeq 4.3$ Å. Such a large chain-end region could accommodate amorphous material consisting of shorter chains and ester chains which do not bridge the amorphous region. The fact that a similar structure is not formed by Mm3, consisting of *n*-alkanes only, emphasises the important role of hydrogen bonding in the structure of this plant wax.

The melting transition of *Hordeum vulgare* wax is ~18 K higher than that of Mm1 (and Mm3) and ~13 K lower than that of Mm2. This observation is compatible with the proposed structural model. The bridging of adjacent layers of short chains and the intermolecular hydrogen bonds within a layer should result in a melting transition at a temperature higher than that of the monolayered Mm1.

Since the average chain-lengths of plant waxes lie within the short chain-length distribution, an increase in the percentage of short chains results in a decrease in the chain-length distribution ($\sigma$ in Table 2). Therefore, the effect of steric hindrances should be decreased and the crystallinity increased. Figure 7 shows the experimentally determined dependence of the crystallinity of three plant waxes as a function of the percentage of chains belonging to the short chain-length component. It is clear that an increase in the fraction of short chains results in an increase in the crystallinity.

Since some of the wax is embedded within the matrix of the cuticle, it is possible that weak van der Waals forces and stronger hydrogen bonds exist between the wax and the -OH and -COOH groups of the cutin polymer. This is a surface effect which should not influence the bulk of the wax.

## 4 Conclusions

The presence of intermolecular hydrogen bonding in *Hordeum vulgare* wax influences the structure of the wax in three major ways. Firstly, phase separation of the shorter and longer chains is prevented by bridging of adjacent layers of shorter chains by longer chains. Bridging does not occur in the absence of hydrogen bonding. Secondly, hydrogen bonding between chains with different structures results in a relatively large amorphous zone. Reynhardt and Riederer (1994) emphasised the importance of the crystalline and amorphous zones of plant waxes in regulating the diffusion of molecules across the transport barrier. Owing to the absence of a discrete structural order, the amorphous zone is accessible to permeating molecules, which can easily diffuse in this material of relatively high fluidity. On the other hand, the crystalline zone excludes molecules diffusing across the barrier. Thirdly, due to intermolecular hydrogen bonding, the melting point of the wax is considerably higher than that of a mixture of *n*-alkanes with a similar chain-length distribution.

**Acknowledgements** Financial support from the Research and Bursaries Committee of the University of South Africa is acknowledged.

## References

Basson I, Reynhardt EC (1992a) Defect chain motions in the low temperature phase of multiple mixtures of n-alkanes by means of nuclear magnetic resonance spin-lattice relaxation time measurements. J Chem Phys 97:1287–1295

Basson I, Reynhardt EC (1992b) The structure and melting of paraffinic Fischer-Tropsch waxes. Chem Phys Lett 198:367–372

Baker EA (1982) Chemistry and morphology of plant epicuticular waxes. In: Cutler DF, Alvin KL, Price CE (eds) The plant cuticle. Academic Press, London, pp 139–165

Craig SR, Hastie GP, Roberts KJ, Sherwood JN (1994) Investigation into the structure of some normal alkanes within the homologous series $C_{13}H_{28}$ to $C_{60}H_{122}$ using high-resolution synchrotron x-ray powder diffraction. J Mater Chem 4:977–981

Holloway PJ (1982) Structure and histochemistry of plant cuticular membranes. In: Cutler DF, Alvin KL, Price CE (eds) The plant cuticle. Academic Press, London, pp 45–85

Kolattukudy PE (1980) Bio-polyester membranes of plants – cutin and suberin sources. Science 208:990–1000

Le Roux JH, Loubser NH (1980) Nuclear magnetic resonance investigation of the mobile phase in paraffinic Fischer-Tropsch waxes. SA J Sci 76:157–161

Nyburg SC, Potworowski JA (1973) Prediction of unit cells and atomic coordinates for the n-alkanes. Acta Crystallogr B29:347–352

Reynhardt EC (1985a) NMR investigation of Fischer-Tropsch waxes: II. Hard wax. J Phys D (Appl Phys) 18:1185–1197

Reynhardt EC (1985b) NMR investigation of Fischer-Tropsch waxes: III. $^{13}C$ and $^{1}H$ study of oxidized hard wax. J Phys D (Appl Phys) 18:2519–2528

Reynhardt EC (1986) Temperature dependence of the cell parameters of Fischer-Tropsch waxes: Hard wax and oxidized hard wax. J Phys D (Appl Phys) 18:1925–1938

Reynhardt EC, Riederer M (1991) Structure and molecular dynamics of the cuticular wax from leaves of *Citrus aurantium* L. J Phys D (Appl Phys) 24:478–486

Reynhardt EC, Riederer M (1994) Structures and molecular dynamics of plant waxes: II. Cuticular waxes from leaves of *Fagus sylvatica* L. and *Hordeum vulgare* L. Eur Biophys J 23:59–70

Riederer M, Schneider G (1990) The effect of the environment on the permeability and composition of citrus leaf cuticles. 2. Composition of soluble cuticular lipids and correlation with transport properties. Planta 180:154–165

Schneider J (1987) Rietveld method runs on IBM-AT. Acta Cryst A43, Suppl C:295

Stokhuyzen R, Pistorius CWFT (1970) Phase behaviour of Fischer-Tropsch wax fractions under high pressure. J Appl Chem 20:1–6

Vainshtein BK (1966) Diffraction of x-rays by chain molecules. Elsevier Publishing Company, Amsterdam, pp 35–108